Journal of the European Ceramic Society 13 (1994) 211–219

Sintering of Wet-Milled Centrifugal Cast Alumina

P. Hidber, F. Baader, Th. Graule & L. J. Gauckler

Nichtmetallische Werkstoffe, Eidgenössische Technische Hochschule, ETH Zentrum, CH-8092 Zürich, Switzerland

(Received 3 September 1993; accepted 10 October 1993)

Abstract

Properties of water based alumina suspensions prepared by attrition milling were studied. Pore size distributions and sintering behavior of centrifugal cast green compacts produced from such suspensions are reported.

Attrition milling is very effective in deagglomerating the starting powder, resulting in suspensions almost free of agglomerates. However, an increasing amount of $Al(OH)_3$ is formed with increasing attrition time. The $Al(OH)_3$ content in the suspension as well as in the green compact was found to increase linearly with milling time. Whereas the $Al(OH)_3$ did not change green densities (68% TD) remarkably, the mean pore size of the green compacts decreased by 40% and shrinkage during sintering was strongly affected. During heating, the transformation of $Al(OH)_3$ to α-Al_2O_3 caused pore growth, which severly delayed and disturbed the densification process and therefore lowered the final sintered densities.

Removal of the $Al(OH)_3$ from the suspension by an acid washing step after the attrition milling led to a fully dense, submicrometer grained α-Al_2O_3 at 1400°C sintering temperature.

Der Einfluß des Attritormahlens auf die Eigenschaften wässriger Aluminiumoxidsuspensionen wie auch Porengrößenverteilung und Sinterverhalten der mittels Zentrifugalschlickerguß hergestellten Grünkörper wurde untersucht.

Attritormahlen ist ein effektives Mittel zum Aufbrechen der im Ausgangspulver enthaltenen Agglomerate. Mit zunehmender Mahldauer wird jedoch eine beträchtliche Menge an $Al(OH)_3$ gebildet. Der $Al(OH)_3$-Gehalt in der Suspension wie auch in den über Zentrifugalschlickerguß hergestellten Grünkörpern steigt linear mit der Mahldauer. Während das $Al(OH)_3$ keinen nennenswerten Einfluß auf die Gründichten (68% TD) zeigt, nimmt der mittlere Porenradius in den Grünkörpern um 40% ab, ebenso wird der Sinterprozeß stark beeinträchtigt. Das beim Aufheizen durch die Umwandlung von $Al(OH)_3$ zu α-Al_2O_3 verursachte Porenwachstum verzögert den Sinterprozeß beträchtlich und bewirkt eine Abnahme der Enddichte.

Durch die Abtrennung des während des Attritormahlens gebildeten $Al(OH)_3$ mittels einer Säurewäsche gelingt es, ein vollkommen dichtgesintertes, feinkörniges α-Al_2O_3 bei 1400°C Sintertemperatur herzustellen.

Nous avons étudié l'influence de l'attrition sur les propriétés des suspensions aqueuses d'oxyde d'aluminium (Al_2O_3) ainsi que sur la distribution de la taille des pores et le comportement au frittage des pièces vertes préparées par coulage centrifuge à partir de ces suspensions.

L'attrition est une méthode efficace pour éliminer les agglomérats présents dans les poudres. Cependant en augmentant la durée d'attrition il se forme une quantité croissante d'hydroxyde d'aluminium, $Al(OH)_3$. Le contenu d'$Al(OH)_3$ dans la suspension et dans la pièce verte préparée par coulage centrifuge augmente linéairement avec la durée d'attrition. Alors qu'$Al(OH)_3$ n'influence pas la densité verte (68% TD), le rayon moyen des pores de la pièce verte diminue d'environ 40%, ce qui freine le processus de frittage. Pendant le frittage la croissance des pores engendrées par la transformation $Al_2O_3 \rightarrow Al(OH)_3$ ralentit le processus de densification et entraîne une diminution de la densité frittée.

Par un lessivage à l'acide de la poudre, on élimine $Al(OH)_3$ formé lors de l'attrition pour obtenir, après frittage à 1400°C, des échantillons denses d'Al_2O_3 démontrant une microstructure submicronique très fine.

1 INTRODUCTION

The production of high density ceramics requires the use of fine, agglomerate free powders. There

Journal of the European Ceramic Society 0955-2219/94/$7.00 © 1994 Elsevier Science Limited, England. Printed in Great Britain

fore, powders must be pretreated before shaping by some technique such as ball or attrition milling to eliminate agglomerates.[1] Although it is well known that the physicochemical environment has a large influence on the comminution process,[2-6] and that grinding aids can improve the grinding efficiency,[7-9] milling is usually considered to be a simple comminution process resulting in changes of the agglomerate and particle size distribution. However, in some cases it is possible to induce or enhance either solid state reactions, such as phase transformations and amorphization,[10-13] or reactions between the powder and the liquid used in the wet milling operations.[1,10,14] Alpha alumina for example is known to react both with organic liquids[14] and water[1], respectively. In an aqueous medium, the formation of an aluminium monohydrate layer on α-Al_2O_3 particles has been observed.[1] This hydration process, which can be mechanically activated, is due to the thermodynamical instability of α-Al_2O_3 in water.[15] By attrition during the wet milling process, the aluminium monohydrate layer is continuously removed from the surface and aluminium ions are released from the particles into the water.[1]

Depending on the pH of the suspension and the aluminium concentration, various species of aluminium hydroxides exist in the solution (Fig. 1). The unhydrolyzed Al^{3+} is stable below pH 3. With increasing pH, the Al^{3+} ion hydrolyzes and condenses, forming a variety of positively charged mono- and polynuclear complexes.[16] Many of these large polynuclear hydroxides and oxo hydroxides can be stable indefinitely, but are in fact metastable with respect to the precipitation of $Al(OH)_3$.[16] Above pH 9, the $[Al(OH)_4^-]$ is the predominant species. Between pH 5 and 8, almost no aluminium is dissolved, since the only existing species, the uncharged $Al(OH)_3^0$, is nearly insoluble. In addition to transient amorphous precipitates, γ-$Al(OH)_3$ and α-$Al(OH)_3$ can occur which hereafter will be summarized by the term '$Al(OH)_3$'.

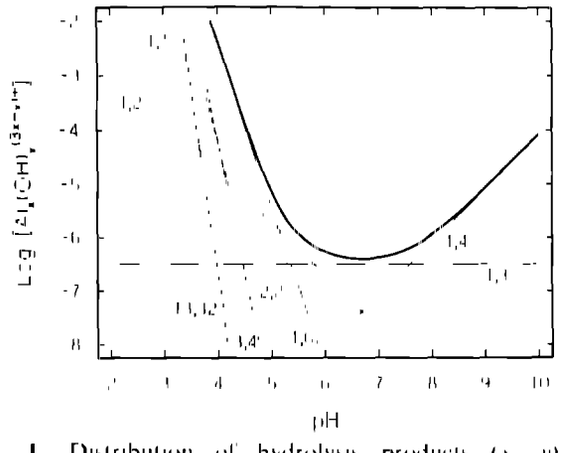

Fig. 1. Distribution of hydrolysis products (○, ▫) in $[Al_x(OH)_y]^{(3x-y)+}$ at an ionic strength I = 1 and at 25°C in solutions saturated with α-$Al(OH)_3$.[16]

The transformation of $Al(OH)_3$ to α-Al_2O_3 during drying and sintering has been the subject of an extensive literature.[15,17-29] Generally, the transformation sequence for aluminium hydroxide upon heating is

$$\text{amorphous}/\alpha/\gamma\ Al(OH)_3 \rightarrow \gamma/\alpha\ AlO(OH) \rightarrow \gamma/\delta/\theta\ Al_2O_3 \rightarrow \alpha\ Al_2O_3$$

The sequence of the transition forms is controlled by the structure of the starting material.[24] The rate and temperature of the transformation to α-Al_2O_3 can be influenced by seeding the aluminium hydroxides as well as the transition aluminas (hereafter simply, if somewhat inaccurately, referred to as 'γ-Al_2O_3') with additives such as α-Al_2O_3[24,25] or α-Fe_2O_3[19,26,29] particles. The transformation is connected with a dramatic increase of the density, from 2.42 g/cm^3 (gibbsite) to 3.986 g/cm^3 (corundum). In addition, the crystal system changes from monoclinic (gibbsite, bayerite) to hexagonal (corundum).[24] Therefore, if $Al(OH)_3$ is present in a green compact prior to sintering, it will have a detrimental effect on the sinterability, the density and the microstructure of the sintered compacts.[15]

Previous studies investigated the influence of attrition milling on the particle size reduction rates as well as on the particle size distribution.[10,11] However, little attention was paid to the fact that the powder particles can experience enhanced hydrolysis during milling.

Therefore, this investigation was designed to elucidate the effect of attrition milling of alumina suspensions with regard to the formation of aluminium hydroxide. In addition, the influence of this aluminium hydroxide on the green body properties was characterized as well as the sinterability and the microstructure. Centrifugal casting was used as a green body forming technique. To be able to separate the influence of (a) $Al(OH)_3$ and (b) changes of the particle size on the microstructure of green and sintered compacts, a fine alumina powder was chosen, which will undergo almost no further particle reduction during milling. A method is shown on how to prepare hydroxide free, good sinterable green compacts even if attrition milling is used for the deagglomeration and suspension preparation step.

2 EXPERIMENTAL PROCEDURES

2.1 Suspension preparation

All experiments were carried out using a dry milled high purity (>99.99%) α-Al_2O_3 powder (RCHP DBM, Reynolds Aluminum Co., Bauxite,

Arkansas 72011, USA) with a specific surface area of 8.59 m^2/g and a mean particle size of 0.3 μm. Suspensions with 80wt% solid and pH 4.3 were prepared using high purity water (specific electrical resistance of 20 MΩcm) and concentrated nitric acid (p.a., Merck, 6100 Darmstadt Germany) or NH_4OH (puriss Fluka, 9470 Buchs, Switzerland) for pH adjustment.

Milling was performed with an attrition mill (Molinex PE 075, Netzsch Feinmahltechnik GmbH 8672 Selb, Germany). Grinding media (spheres 3mm diameter) as well as the cylindrical grinding chamber (0.08 m in diameter × 0.1 m in length) were of dense αAl_2O_3 (99.5 % pure). Media (0.700 kg) and suspension (0.450 kg) loadings were kept constant for all experiments. The rotor was operated at 1800 rpm. During milling pH was controlled and, if necessary, readjusted by addition of nitric acid. Milling time was the only variable. The wear of the milling media was below 0.2wt% (60 min milling).

Samples for particle size analysis were drawn during milling after 0, 5, 15, 30 and 60 min. The particle size distributions were measured using light scattering methods (Microtrac UPA FRA, series 9200, Leeds & Northrup, North Wales, PA 19454, USA).

Rheological characteristics of the suspensions were determined using a rotating viscosimeter (Rheomat 115A, Mettler Toledo AG, 8606 Greifensee, Switzerland). To prepare aluminium hydroxide free compacts, the suspended alumina powder was washed three times, first with 0.5M HCl, then twice with water. Prior to the centrifugal casting of the samples, the pH was readjusted to 4.2.

2.2 Casting and green body characterization

Green bodies were prepared by centrifugation of 0.080 kg alumina suspension at 4000 g for 90 min (centrifuge Hermle ZK 510, B. Hermle GmbH, 7209 Gosheim, Germany). After an appropriate dilution with 0.1N HCl, the aluminium concentration in the supernatant was determined by atomic absorption spectroscopy (AAS) (AA Spectrometer, Instrumentation Laboratory Inc., Wilmington, MA 01887, USA) after the clear supernatant solution had been centrifuged for another 90 min at 5000 g. Green density was determined by the Archimedes method. The immersion medium was mercury. All green bodies for Hg porosimetry (Porosimeter 2000, Carlo Erba Strumentazione, Milan, Italy) were dried at 120°C for 8 h. DTA/TG measurements were performed in air (heating rate 10 K/min) on a Mettler Thermoanalyzer TA1 (Mettler Toledo AG, 8606 Greifensee, Switzerland).

2.3 Sintering process

The comparison of the sinterability of the different treated powders was performed by dilatometric studies (Bahr 802 S, Bahr Geratebau GmbH, 4971 Hullhorst, Germany). The heating rate was 5 K/min, the cooling rate −50 K/min. The maximum sintering temperature (1570°C) was held for one hour.

Isothermal sintering was performed with green compacts heated in air at a constant rate of 60 K/h to 1400°C and held at this temperature for 2 h (cooling rate 400 K/h).

The microstructural development of green bodies made up from washed and unwashed powder suspensions was studied by heating the compacts with a constant heating rate (5 K/min) to 1400°C. When the maximum temperature was reached, the compacts were air quenched. The polished and thermally etched surfaces (1350°C for 30 min) were examined by scanning electron microscopy (Jeol JSM 6400A, Jeol Ltd, Tokyo, Japan).

2.4 Simulation of the aluminium hydroxide influence

The influence of aluminium hydroxide on the sintering behaviour was simulated by adding 7.5wt% $AlCl_3 6H_2O$ (crystalline, Merck, 6100 Darmstadt, Germany) to an alumina suspension with 65wt% solid. This $AlCl_3$ concentration corresponds to 1.2wt% $Al(OH)_3$ after hydrolysis or an Al(III) concentration in the solution of 0.31 mol/litre. The pH was adjusted to 4.2 by the addition of NH_4OH. After 4 min ultrasonication (Vibra Cell VC600, Sonics and Materials Inc., Danbury, USA), the samples were treated as described in Sections 2.2 and 2.3.

3 RESULTS

3.1 Attrition milling of the alumina suspension

To investigate the formation of aluminium hydroxide during wet milling, 80wt% alumina suspensions at pH 4.2 were attrition milled for different times. This relatively high powder loading was chosen to minimize the wear of the grinding media.[10,11] The particle size distributions for the milled samples are shown in Fig. 2. As expected for such a fine powder, the mean particle size is not much affected by the milling process. However, agglomerates larger than 1 μm are very efficiently destroyed.

The aluminium concentration in the dispersion medium as a function of the grinding time is plotted in Fig. 3. As a comparison, the solubility at pH 4.2 of amorphous $Al(OH)_3$, the most soluble form of all aluminium hydroxide species,[9] is also shown. Suspending the alumina powder in water leads to an aluminium concentration of 0.045 mol/

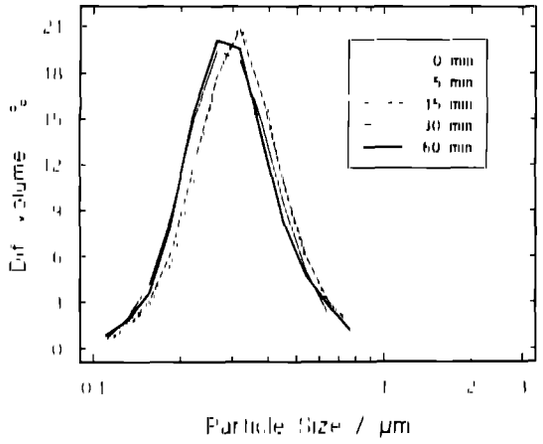

Fig. 2. Effect of attrition milling time on the particle size distribution

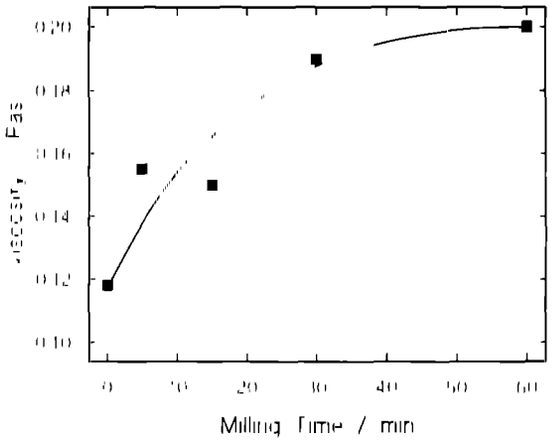

Fig. 4. Viscosity (shear rate 99/s) of the alumina suspensions as a function of milling time at 25°C

litre. During milling, the aluminium concentration increases almost linearly to a final value of 0.63 mol/litre, which is far above the theoretical solubility of $Al(OH)_3$ at this pH.

In Fig. 4, the viscosity (shear rate 99/s) of the suspensions is plotted versus the milling time. Starting from 0.11 Pas, it increases with growing aluminium concentration in the suspensions to 0.2 Pas after 60 min milling time.

3.2 Green compact characterization

After attrition milling, compacts were prepared by centrifugal casting of the suspensions. The pore size distributions of the dried green compacts were measured by Hg intrusion porosimetry. Green densities and mean pore radii of the compacts versus milling time are plotted in Fig. 5. The maximum green density (68.3% ρ_{th}) is achieved after 30 min grinding time. Prolonged milling results in a slight decrease of the density.

The mean pore radius decreases from 42nm to 29 nm after 30 min. Further attrition milling leads to an increase of the pore radius. The minimum of the mean pore radius coincides with the maximum of the green density.

In Fig. 6, the $Al(OH)_3$ content in the green compacts is correlated with the weight loss during sintering, varying from 0.8wt% (0 min milled) to 1.1wt% (60min milled), which corresponds to 2.5 and 3.2 wt% $Al(OH)_3$, respectively. According to TG measurements, 95% of the weight loss occurs between 120°C and 600°C, which is in good agreement with the temperature range of the decomposition of $Al(OH)_3$ to γ-Al_2O_3.[13] This weight loss is therefore attributed mainly to the oxide formation.

3.3 Sintering kinetics of green compacts with $Al(OH)_3$

The shrinkage rate curves for the centrifugal cast compacts are plotted in Fig. 7. Generally, the longer the powder is milled, the more the densification process is disturbed. Additionally, prolonged milling of the alumina powder results in a bimodal shrinkage rate distribution. With increasing grinding time and thus with increasing $Al(OH)_3$ content in the green compact, the first maximum of the shrinkage rate versus temperature curve shifts from 1380°C to 1300°C. Compacts with higher γ-Al_2O_3 contents showed lowered shrinkage

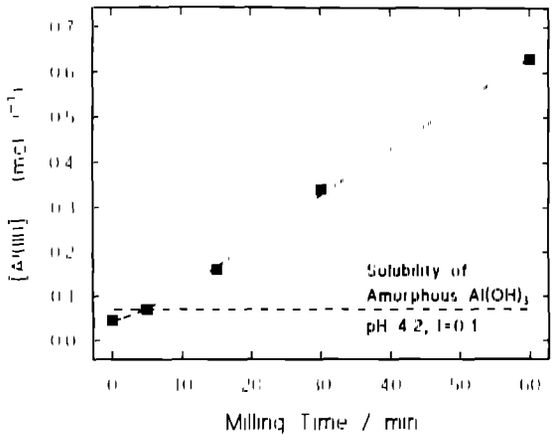

Fig. 3. Aluminium concentration in the dispersion medium as a function of the attrition milling time. The solubility of amorphous $Al(OH)_3$, the most soluble of all aluminium hydroxide species, is also shown (pH 4.2, I = 0.1).[13]

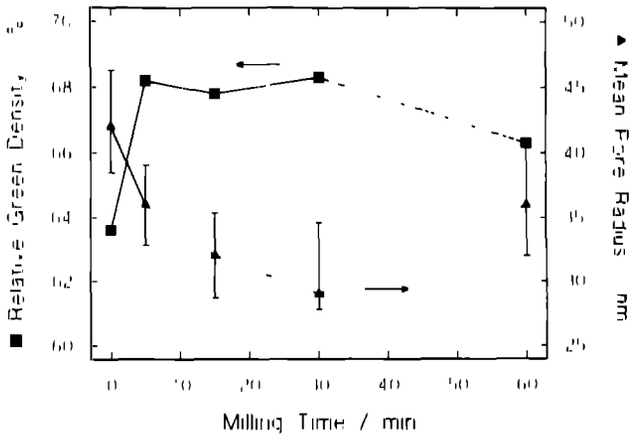

Fig. 5. Green density and mean pore radius as a function of milling time. Bars represent pore size distribution width (d_{75} and d_{25}, respectively).

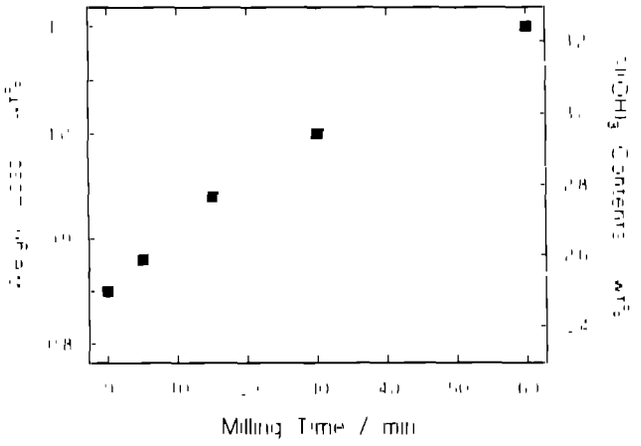

Fig. 6 Weight loss of the compacts during heating up to 1200°C as a function of milling time

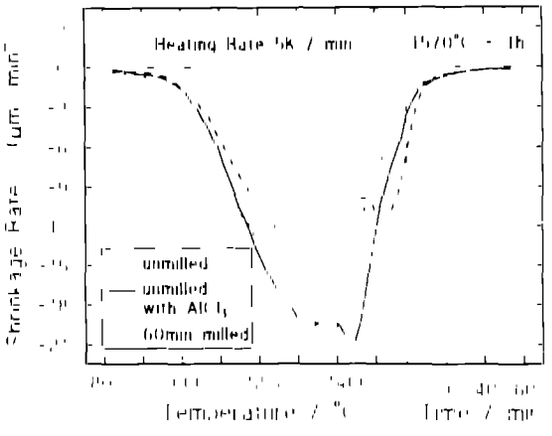

Fig. 8 Shrinkage rates for centrifugal cast compacts (a) unmilled (b) unmilled with addition of $AlCl_3$ and (c) milled for 60min (normalized on a compact length of 0.01m)

rates, indicating that densification is retarded by parallel occurring processes. From density data versus time, it is obvious that compacts of the powders milled for a longer time density only at considerably higher temperatures. This also becomes evident for the 60 min treated powder, which shows a pronounced second maximum at 1500°C. This second shrinkage rate maximum is hardly visible after 0 and 5 min of attrition, but becomes more and more pronounced with increasing milling time. In addition, the longer the alumina powder is milled, the higher is the residual shrinkage rate during the isothermal sintering period at 1570°C.

The sintering behaviour of the samples milled for a long time is mainly influenced by the presence of $Al(OH)_3$. In Fig. 8 the shrinkage rate curves of the 0 and 60 min milled samples are plotted in comparison with an unmilled sample, to which $Al(OH)_3$ was added in the form of 7.5wt% aluminium chloride. This corresponds to 1.2wt% $Al(OH)_3$ after hydrolysis or an aluminium concentration of 0.31 M. Thus this latter compact has the same particle size distribution as the unmilled compact, but an $Al(OH)_3$ content comparable to a sample milled for a long time. As expected for a compact with this amount of $Al(OH)_3$ the shrinkage rate curve has two maxima. The first maximum at 1330°C is comparable to the one of the 0 and 5 min milled samples and the second at 1440°C is only little lower than the one found with prolonged milling. This result clearly shows that the appearance of these two maxima is caused by the $Al(OH)_3$ in the powder compacts.

The final densities (1400°C/2h) are in the range of 99.2% ρ_{th} for 0 and 5 min milling time and decrease to 94.8% ρ_{th} for samples attrition milled for 60 min (Table 1). It is worth noting that it is not the green body with the highest density and the smallest mean pore size but rather the one with the lowest green density and the largest mean pore size that achieved the highest final density.

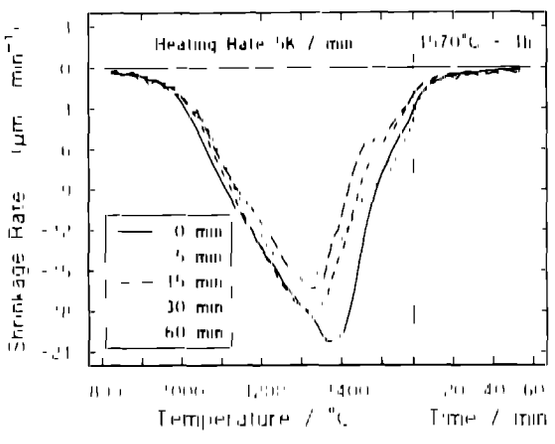

Fig. 7. Influence of the milling time on the shrinkage rates of the centrifugal cast compacts (normalized on a compact length of 0.01m)

3.4 Sintering kinetics of green compacts without $Al(OH)_3$

In order to benefit from attrition milling as a method to break up agglomerates and to reduce the particle size, the $Al(OH)_3$ formed by the milling process, has to be removed. An efficient technique to separate $Al(OH)_3$ from α-Al_2O_3 is acidic washing of the powder.

$Al(OH)_3$ free compacts from the 30 min milled alumina suspension were prepared by repeating the acidic washing of the powder three times prior

Table 1 Evolution of the final density with milling time

Milling time (min)	*Density (unwashed)* g/cm³	% ρ_{th}	*Density (washed)* g/cm³	% ρ_{th}
0	3.953	99.2		
5	3.953	99.2		
15	3.941	98.9		
30	3.901	97.9	3.982	99.9
60	3.780	94.8		

Table 2. Characteristics of hydroxide containing (unwashed) and hydroxide free (washed) samples, both milled for 30 min

	Hydroxide containing	*Hydroxide free*
[Al(III)] in the water (mol/litre)	0.39	0.025
Mean pore radius in the green body (nm)	29	35
Green density (g/cm^3)	2.72 (68.8 %ρ_{th})	2.68 (67.2 %ρ_{th})
Temperature of maximum shrinkage (°C)	1290/1500	1290
Final density (g/cm^3)	3.901 (97.9 %ρ_{th})	3.982 (99.9 %ρ_{th})

to centrifugal casting. A comparison of the properties of compacts made from washed and unwashed powders is given in Table 2. The hydroxide free green body has a 20% larger mean pore radius and a 1% lower green density than the hydroxide containing sample. The shrinkage and shrinkage rate curves for both materials show a peak at 1290°C (Fig. 9). The hydroxide free compacts show neither a second sintering maximum nor a significant shrinkage rate during the isothermal final stage of sintering, which means that the body has reached its final density (3.982 g/cm^3 or 99.9 %ρ_{th}) at the beginning of the isothermal final stage of sintering.

The development of the pore size distribution during the constant heating rate sintering phase with increasing temperature for both the unwashed and washed compacts is plotted in Figs. 10(a) and (b). At 100°C, the mean pore radius of the unwashed sample is about 15% smaller than the one of the washed body (30 nm versus 35 nm). Apart from a slight pore growth, the pore size distribution as well as the pore volume of the washed compact remains unaffected up to 1000°C. At higher temperatures, the sintering process leads to a very fast shrinkage of the pore sizes. Above 1300°C, no open porosity remains. In contrast to the behaviour of the washed compact, the unwashed sample exhibits a considerable pore growth up to 1000°C. The mean pore radius is increased by 20%, from 30 nm to 36 nm. Nevertheless, it is still smaller than in the case of the washed compact. With preceding sintering, the pores become smaller, as expected. However, in comparison with the hydroxide free sample, the decrease of the pore size is much slower which is in good agreement with the observed smaller shrinkage rate of the unwashed compact (Fig. 9). A considerable amount of open porosity can be detected even at 1400°C.

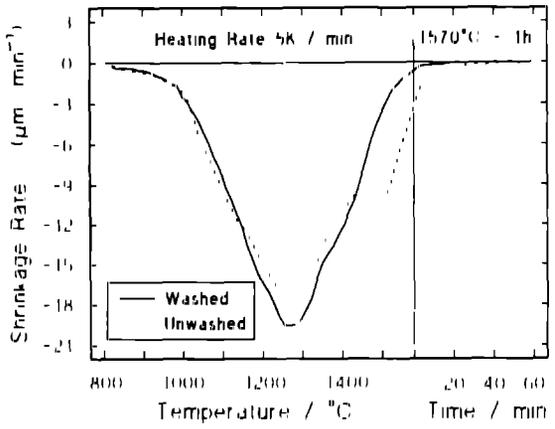

Fig. 9. Shrinkage rates for unwashed and washed compacts (normalized on a compact length of 0.01 m).

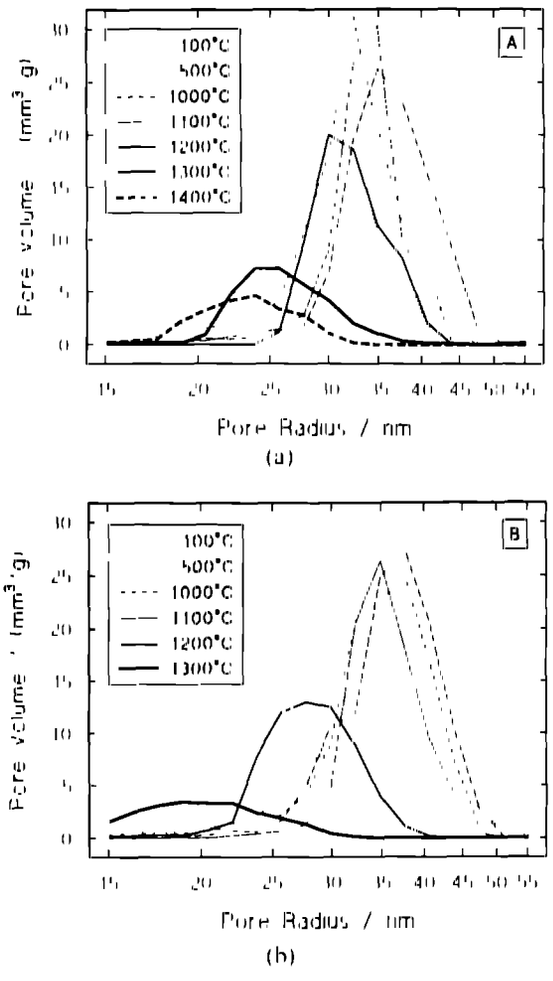

Fig. 10. Pore size distribution of (a) unwashed and (b) washed samples at different temperatures.

The comparison of the microstructures of washed and unwashed compacts (milling time 30 min) heated up to 1400°C (Fig. 11) is a good illustration for the observed pore size and volume development (Fig. 10(a) and (b)). The washed compact has an already very dense, homogeneous microstructure (Fig. 11(a)). In contrast to this fine grained microstructure, the unwashed compacts still exhibit quite a high porosity at this temperature (Fig. 11(b)). Between already dense domains (up to 10 µm), there are many pores (0.2–1 µm) and numerous separations between the grains.

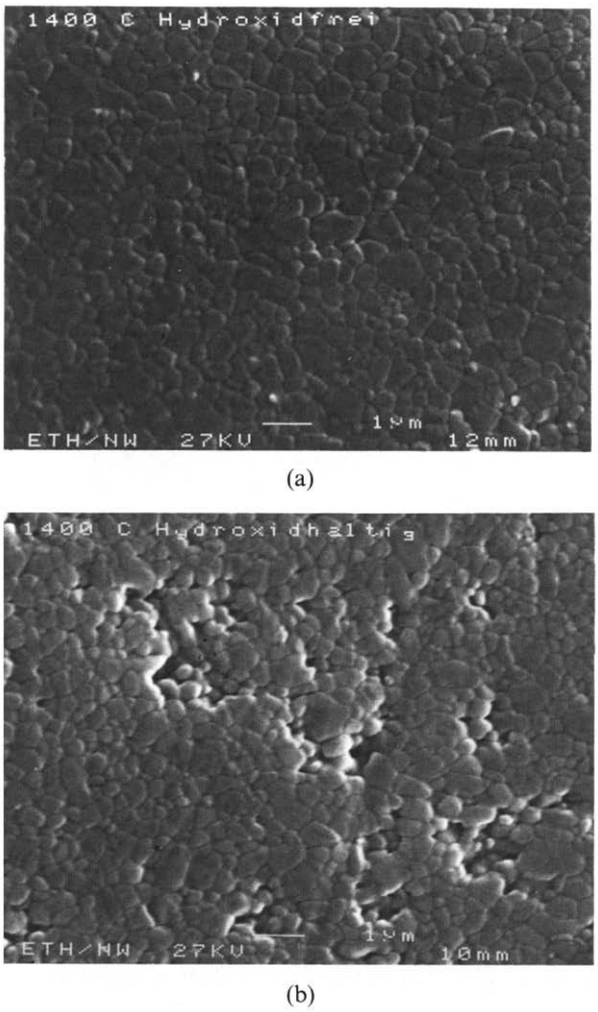

Fig. 11. Microstructure of α Al_2O_3 compacts heated up to 1400°C (a) acid washed powders and (b) unwashed powders

4 DISCUSSION

4.1 Influence of attrition milling on the suspension properties

Attrition milling is known to reduce the amount of agglomerates as well as the particle size very efficiently [10, 11] As expected for such a fine powder, the particle size distribution remains almost unaffected by the milling The main influence of the milling process is the destruction of agglomerates (Fig 2) However, as shown in Fig 3 and Fig 6, the milling is combined with a considerable formation of soluble aluminium species According to Niesz & Bennett[1], the amount of $Al(OH)_3$ formed during milling is increased by the presence of transition aluminas

The aluminium concentration in the supernatant of 0.63 mol/litre after a milling time of 60 min is beyond the solubility reported for gibbsite, bayerite or even amorphous $Al(OH)_3$ at pH 4.2 [16, 12] However, the present case is far from thermodynamical equilibrium Polynuclear aluminium hydroxide or oxo hydroxide complexes, which are formed especially in the case of solutions with high aluminium concentrations, can be stable indefinitely, although they are metastable with respect to the precipitation of $Al(OH)_3$ [16] Therefore, the values in Fig 3 represent not an equilibrium state but the actual total concentration of reactive aluminium (monomeric, polymeric and colloidal species) in the supernatant, which can be acid digested

Although beyond the equilibrium solubility, the aluminium concentration increases linearly with the milling time, which indicates that the mechanically activated water alumina reaction is independent on the aluminium solubility limit in water Therefore, it would also occur if milling was carried out in the pH region of low aluminium equilibrium solubility, e g between pH 5 and 8 (Fig 1)

The increase of the viscosity during milling from 110 mPas to 200 mPas (Fig 4) has three possible causes Firstly, smaller particles immobilize relatively more free water, thus leading to an increase of viscosity [4] Secondly the repulsive force between two similarly charged particles at a fixed zeta potential becomes smaller with decreasing particle size.[11] Since there is almost no change in the particle size distribution after 5 min milling these two mechanisms probably only contribute to the viscosity increase at the beginning of the milling process Thirdly, the increase of the aluminium concentration during the milling process reduces the thickness of the electrical double layer and thereby the repulsive double layer forces [14] As a consequence, the stability of the suspension is reduced, which must result in an increase of the viscosity

4.2 Influence of attrition milling on green and sintered compacts

Centrifugal casting as a shaping method was chosen to exclude influences of the drying and pressing process of the wet milled powders on the sintering behaviour Therefore, all experimental findings concerning the properties of green and sintered compacts have to be discussed in terms of the particle size and the amount of $Al(OH)_3$ in the green compacts, since these parameters are the only variables in this investigation

A model microstructure of the green compact containing $Al(OH)_3$ is shown in Fig 12 The framework of the green body (Fig 12(a)) is built up of interconnected α Al_2O_3 powder particles, which are (at least partially) covered with $Al(OH)_3$ The cavities between the particles are filled with $Al(OH)_3$, which was either not dissolved during the milling process or precipitated during the drying of the compacts The more $Al(OH)_3$ is formed during the wet milling process, the more the pores between the α Al_2O_3 particles are filled with hydroxides, leading to a higher green density

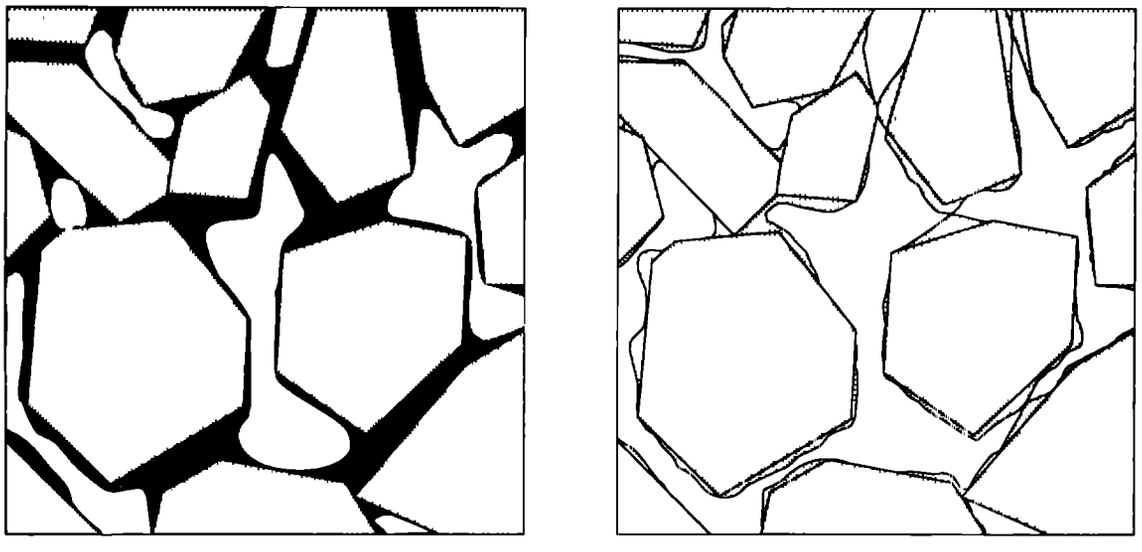

(a) (b)

Fig. 12. Model microstructure of the green body: (a) green compact after casting and drying (at room temperature) and (b) compact after the transformation of $Al(OH)_3$ into α-Al_2O_3 (at ~1200°C). Dark shading, $Al(OH)_3$; light shading, α-Al_2O_3.

and lower mean pore radius (Fig. 5). The large increase of the green density after 5 min milling is probably not a consequence of the described pore filling mechanism, since the $Al(OH)_3$ content in the green compacts increases linearly with the milling time, but rather is due to the break up of the agglomerates. Grinding times longer than 30 min decrease the packing density and increase the pore size, although more $Al(OH)_3$ is available to fill the space between the particles. This should lead to even higher green densities and smaller pore sizes. However, parallel to the $Al(OH)_3$ formation, the suspension's stability is more and more reduced (Section 4.1). This partial coagulation of the suspension impaired the particle packing and leads to more porous compacts with increased pore sizes.

During heating to the sintering temperature, $Al(OH)_3$ transforms into α-Al_2O_3 by a multistep process. These transformations are linked to a volume shrinkage of more than 30%. Consequently, the decomposition of the $Al(OH)_3$ leaves large pores in the microstructure (Fig. 12(b)). At the same time, the very fine transition alumina particles begin to sinter and coarsen at a temperature well below that at which the α-Al_2O_3 matrix begins to shrink. This sintering shrinkage and the volume changes associated with the phase changes should lead to disruption of the particle contacts and a considerable pore growth.[1] In fact, up to 1000°C, the compact with $Al(OH)_3$ undergoes a considerable pore growth. Above 1000°C, this process is countered by the beginning of sintering. Further pore growth due to the described mechanism is suppressed. However, since the microstructure is strongly disturbed—especially the particle–particle contacts, the densification process is retarded, which can be inferred from the appearance of a second sintering maximum in the graph of shrinkage rate versus temperature (Fig. 7). As expected, the pore size distribution of the $Al(OH)_3$ free sample is almost unaffected up to 1000°C. Although the medium pore size is still larger than that of the unwashed sample, the washed sample can sinter much faster, since the particle–particle contacts are not disturbed by the presence of $Al(OH)_3$. Therefore, it can be fully densified at 1400°C/2h.

5 CONCLUSIONS

(1) Wet attrition milling of alumina not only destroys agglomerates and reduces the mean particle diameter but also leads to $Al(OH)_3$ formation, which is proportional to the milling time. Therefore, milling times should be kept as short as possible. Most of the $Al(OH)_3$ formed is located in the pores of the α-Al_2O_3 matrix.

(2) Upon heating, the $Al(OH)_3$ is transformed by several steps to α-Al_2O_3, leaving large pores and disruption of particle–particle contacts in the microstructure. This damage of the microstructure results in a reduced shrinkage rate, a bimodal shrinkage rate distribution and a lowering of the final density. The same effect is achieved without milling by addition of an Al(III) salt to an alumina suspension.

(3) Removal of the $Al(OH)_3$ after milling by an acid washing results in the common monomodal shrinkage rate distribution and an enhanced densification.

(4) By a combination of both attrition milling and $Al(OH)_3$ removal, it is possible to get fully dense alumina compacts with a fine, homogeneous microstructure at sintering temperatures as low as 1400°C.

ACKNOWLEDGEMENTS

This work was supported by the Swiss KWF organization under Contract No. 1982.1.

REFERENCES

1. Niesz, D.E. & Bennett, R.B. Structure and properties of agglomerates. In *Ceramic Processing Before Firing*, ed. G.Y. Onoda & L.L. Hench. John Wiley and Sons, New York, 1978, pp. 61–73.
2. Kapur, P.C., Mular, A.L. & Fuerstenau, D.W. The role of fluids in comminution. *Can. J. Chem. Eng.* **43** (1965) 119–124.
3. Somasundaran, P. & Lin, I.J. Effect of the nature of environment on comminution processes. *Ind. Eng. Chem. Process Des. Develop.* **11** (1972) 321–331.
4. Somasundaran, P. Theories of grinding. In *Ceramic Processing Before Firing*, ed. G.Y. Onoda & L.L. Hench. John Wiley and Sons, New York, 1978, pp. 105–123.
5. Sacks, M.D. & Khadilkar, C.S. Milling and suspension behavior of Al_2O_3 in methanol and methyl isobutyl ketone. *J. Am. Ceram. Soc.* **66** (1983) 488–494.
6. Sacks, M.D. The influence of the physicochemical environment on wet milling. In *Ultrastructure Processing of Ceramics, Glasses, and Composites*, ed. L.L. Hench & D.R. Ulrich. John Wiley and Sons, New York, 1984, pp. 418–438.
7. Rehbinder, P. New physico-chemical phenomena in the deformation and mechanical treatment of solids. *Nature* **159** (1947) 866–867.
8. Westwood, A.R.C. Tewksbury lecture: control and applications of environment-sensitive fracture processes. *J. Mater. Sci.* **9** (1974) 1871–1895.
9. Sacks, M.D. & Tseng, T. Role of sodium citrate in aqueous milling of aluminum oxide. *J. Am. Ceram. Soc.* **66** (1983) 242–247.
10. Fox, P.G., Mechanically initiated chemical reactions in solids. *J. Mater. Sci.* **10** (1975) 340–360.
11. Lin, I.J., Nadiv, S. & Grodzinski, D.M. Changes in the state of solids and mechano-chemical reactions in prolonged comminution processes. *Minerals Sci. Eng.* **7** (1975) 313–336.
12. Lin, I.J. & Nadiv, S. Review of the phase transformation and syntheses of inorganic solids obtained by mechanical treatment (mechanochemical reactions). *Mat. Sci. Eng.* **39** (1979) 193–209.
13. Kosmac, T. & Courtney, T.H. Milling and mechanical alloying of inorganic nonmetallics. *J. Mater. Res.* **7** (1992) 1519–1525.
14. Dynys, F.W. & Halloran, J.W. Reactions during milling of aluminum oxide. *J. Am. Ceram. Soc.* **64** (1981) C-62–C-63.
15. Carnigha, S.C. Thermochemistry of the aluminas and aluminum trihalides. *J. Am. Ceram. Soc.* **66** (1983) 495–500.
16. Baes, C.F. & Mesmer, R.E. *The Hydrolysis of Cations*. John Wiley and Sons, New York, 1976, pp. 112–123.
17. Badkar, P.A. & Bailey, J.E. The mechanism of simultaneous sintering and phase transformation in alumina. *J. Mat. Sci.* **11** (1976) 1794–1806.
18. Dynys, F.W. & Halloran, J.W. Alpha alumina formation in alum-derived gamma alumina. *J. Am. Ceram. Soc.* **65** (1982) 442–448.
19. Tachida, T., Furuichi, R., Ishii, T. & Itoh, K. The effect of Cr^{3+} and Fe^{3+} ions on the transformation of different aluminum hydroxides to α-Al_2O_3. *Thermochim. Acta* **64** (1983) 337–343.
20. Dynys, F.W. & Halloran, J.W. Alpha alumina formation in Al_2O_3 gels. In *Ultrastructure Processing of Ceramics, Glasses, and Composites*, ed. L.L. Hench & D.R. Ulrich. John Wiley and Sons, New York, 1984, pp. 142–151.
21. Clark, D.E. & Lannutti, J.J. Phase transformations in sol-gel derived aluminas. In *Ultrastructure Processing of Ceramics, Glasses, and Composites*, ed. L.L. Hench & D.R. Ulrich. John Wiley and Sons, New York, 1984, pp. 126–141.
22. Raman, S.V., Doremus, R.H. & German, R.M. Characterization and initial sintering of a fine alumina powder. In *Sintering and Heterogeneous Catalysis* **16**, ed. G.C. Kuczynski, A.E. Miller & G.A. Sargent. Plenum Press, New York, 1984, pp. 253–264.
23. Wefers, K. & Misra, C. Oxides and hydroxides of aluminum. Alcoa Technical Report No. 19, revised, 1987.
24. Kumagai, M. & Messing, G.L. Controlled transformation and sintering of a boehmite sol-gel by α-alumina seeding. *J. Am. Ceram. Soc.* **68** (1985) 500–505.
25. Shelleman, R.A. & Messing, G.L. Liquid-phase-assisted transformation of seeded γ-alumina. *J. Am. Ceram. Soc.* **71** (1988) 317–322.
26. McArdle, J.L. & Messing, G.L. Transformation and microstructure control in boehmite-derived alumina by ferric oxide seeding. *Adv. Ceram. Mater.* **3** (1988) 387–392.
27. Descamond, M., Brodhag, C. & Thevenot, F. Sinterability of γ-phase containing alumina powders. In *Proceedings of the Second International Conference Ceramic Powder Processing Science*, ed. H. Hausner, G.L. Messing & S. Hirano. Deutsche Keramische Gesellschaft, Koln, 1989, pp. 705–712.
28. Chou, T.C. & Nieh, T.G. Nucleation and concurrent anomalous grain growth of α-Al_2O_3 during γ–α phase transformation. *J. Am. Ceram. Soc.* **74** (1991) 2270–2279.
29. McArdle, J.M. & Messing, G.L. Transformation microstructure development and densification in α-Fe_2O_3 seeded boehmite-derived alumina. *J. Am. Ceram. Soc.* **76** (1993) 214–222.
30. Beckers, G.J. & Correia, L.A. Attrition milling of alumina to submicron sizes. In *Ceramic Transactions, 12 Ceramic Powder Science III*, ed. G.L. Messing, S. Hirano & H. Hausner. American Ceramic Society, Columbus, OH, 1990, pp. 191–199.
31. Kerr, M.G. & Reed, J.S. Comparative grinding kinetics and grinding energy during ball milling and attrition milling. *Am. Ceram. Soc. Bull.* **71** (1992) 1809–1816.
32. Lindsay, L.W. & Walthall, P.M. The solubility of aluminum in soils. In *The Environmental Chemistry of Aluminum*, ed. G. Sposato. CRC Press Inc., Boca Raton, Florida, 1989, pp. 221–239.
33. Hirata, Y., Nakagama, S. & Ishihara, Y. Calculation of interaction energy and phase diagram for colloidal systems. *J. Ceram. Soc. Japan, Int. Edition* **98** (1990) 333–338.
34. Israelachvili, J., *Intermolecular & Surface Forces (second edition)*. Academic Press, London, 1991, p. 238.